2+1 resonantly enhanced multiphoton ionization of CO via the $E\,^1\Pi$–$X\,^1\Sigma^+$ transition: From measured ion signals to quantitative population distributions

Melissa A. Hines, Hope A. Michelsen, and Richard N. Zare
Department of Chemistry, Stanford University, Stanford, California 94305

(Received 9 July 1990; accepted 16 August 1990)

The 2 + 1 resonantly enhanced multiphoton ionization (REMPI) spectrum of the CO $E\,^1\Pi$–$X\,^1\Sigma^+$ (0,0) transition is used to determine ground state rotational populations with a detection sensitivity of approximately 3×10^6 molecules per quantum state per cm^3. Low rotational states of CO are ionized to CO^+; however, high rotational states form both C^+ and CO^+. This effect is shown to be both branch dependent and J dependent. In order to extract reliable ground state populations, both the C^+ and CO^+ channels must be measured. When the C^+ channel is not accounted for, high rotational states are systematically undercounted. New rotational constants are determined for the $C^{12}O^{16}$ $E\,^1\Pi$ state; B_0^f is 1.9526 cm^{-1} and B_0^e is 1.9645 cm^{-1}. The large lambda doubling ($q = 0.0119\ cm^{-1}$) of the E state is attributed to a perturbation by the nearby $C\,^1\Sigma^+$ state.

I. INTRODUCTION

Because carbon monoxide (CO) is one of the simplest carbon-containing molecules, it plays an important role in many fields, including surface science. Much effort has therefore been expended in developing a sensitive and quantitative method for detecting CO in its ground electronic state ($X\,^1\Sigma^+$) with quantum state resolution. The need for sensitivity is probably most apparent in surface studies. These experiments are almost always carried out in an ultrahigh vacuum environment in order to maintain a clean surface. A background pressure of only 10^{-6} Torr could completely cover a surface in seconds. To date such experiments have been hampered (but not halted![1,2]) by the lack of a CO detection technique with adequate detection sensitivity.

The most obvious spectroscopic method involves infrared absorption or emission. Because of the inherent problems with background radiation, direct absorption is not very amenable to minute densities. Since the rate of spontaneous emission is proportional to the cube of the frequency, states that emit in the infrared have a very long lifetime. This long lifetime, combined with the relatively poor detection efficiency of infrared detectors, makes infrared fluorescence a rather unsatisfactory technique.

One way to overcome the lifetime problems of infrared emission would be to use laser-induced fluorescence (LIF) through an excited electronic state of CO. Indeed, this type of detection is much more sensitive than infrared emission. Because the first singlet excited state of CO is approximately 65 000 cm^{-1} above the ground state, this requires either vacuum ultraviolet (VUV) radiation of less than 150 nm or a multiphoton process. VUV LIF of CO via the $A\,^1\Pi$–$X\,^1\Sigma^+$ transition[3] has been shown to have a sensitivity limit (S/N = 1) of 10^6–10^7 molecules per quantum state per cm^3. The detection sensitivity of LIF is, in general, limited by the photon collection efficiency. Great care must be taken in the design of the collection optics and suitable baffling.

The problem of photon collection and detection can be avoided by using resonantly enhanced multiphoton ionization (REMPI). Here ions are produced, and it is quite easy to attain a detection efficiency near unity for ions. If a suitable resonant state is chosen, full quantum state resolution may be obtainable. Although REMPI detection schemes exist for many molecules, a quantitative scheme with rotational resolution has not been reported for CO.

The 2 + 1 resonantly enhanced multiphoton ionization (REMPI) spectrum of the CO $E\,^1\Pi$–$X\,^1\Sigma^+$ (0,0) transition was first studied by Fujii, Ebata, and Ito.[4] Their study was done on a supersonically cooled jet of CO, so that rotational states above $J = 5$ were not detected. We have extended their work in order to develop a sensitive and quantitative method for the detection of CO. We will show that this REMPI scheme provides full rotational resolution (with the exception of $J = 0$) and can be used to extract rotational populations.

The CO $E\,^1\Pi$–$X\,^1\Sigma^+$ transition has been previously studied using a variety of one-photon techniques. The earliest work was done in absorption by Hopfield and Birge.[5] High-resolution work on the (0,0) band was done in absorption by Tilford, Vanderslice, and Wilkinson[6] and was extended to the (1,0) band by Ogawa and Ogawa.[7]

The $E\,^1\Pi$ state is nominally the $3p\pi$ state, and is considered to be a Rydberg state in a series that converges on the CO^+ $X\,^2\Sigma^+$ state. The E state lies approximately 93 000 cm^{-1} above the ground state, which is 0.29 eV above the $C(^3P) + O(^3P)$ adiabatic dissociation limit. This has hampered fluorescence studies of this state, because predissociation is favored over fluorescence by a factor of 9.[8] The lifetime of the E state has been measured as 1.5 ns.[9]

II. EXPERIMENTAL

Light for this experiment was generated by a 10 Hz Nd:YAG pumped dye laser at approximately 645 nm and a

 0021-9606/90/248557-08$03.00

bandwidth $\geqslant 0.05\ \mathrm{cm}^{-1}$. The dye laser oscillator was a modified Littman cavity (Pegasus Enterprises) and was amplified by a three-stage amplifier. Ultraviolet (UV) light of approximately 215 nm was produced by first doubling the output of the dye laser in KD*P and then mixing the resulting UV light with the residual fundamental in β-BaB_2O_4 to effect a net tripling. Typically, 85 mJ of fundamental light produced approximately 3 mJ of tripled light. All laser powers quoted in this paper were measured with a Diamond-Ophir (10A-P-CAL) power meter.

CO was introduced into a UHV chamber (base pressure $\leqslant 2\times10^{-9}$ Torr in this experiment) with a leak valve. Typically, CO partial pressures of 1×10^{-7} Torr, as measured by an (uncorrected) ion gauge, were used to obtain the spectra in this paper. Light was focused into the chamber with either a 300 or a 600 mm FL lens. The resultant ions were accelerated and extracted into a time-of-flight tube, amplified by a CEMA chevron detector (Galileo), and detected with a time-gated ADC (LeCroy 2249SG). Multiple gates were used for simultaneous detection of more than one charge-to-mass ratio. The resulting signal was then collected by an LSI-11/23 minicomputer interfaced to a CAMAC controller. The intensity of a given transition was determined by integrating the ion signal across the line profile.

In contrast to spectroscopic studies performed with a fixed grating and photographic plate, the major source of error in our rotational constants was our inability to calibrate the transition frequencies both accurately and precisely. Our spectra were collected by monitoring the ion signal as a function of time at a constant scan rate. We also monitored the wavelength of the dye laser with an extra-cavity solid etalon and photodiode arrangement. After collecting both the ion signal and etalon signal, we could then correct for scan nonlinearities by performing a linear interpolation to the observed maxima and minima in the etalon signal. The relative wavelengths could be determined in two ways. First, we used a second etalon, which had been calibrated against a hollow cathode Ne lamp with a cw dye laser (Coherent model 599, running broadband with a bandwidth of approximately $1.5\ \mathrm{cm}^{-1}$). Second, we calculated the position of two O and S branch two-photon transitions [e.g., $S(20)$ and $O(20)$] using the high-resolution one-photon transitions of Tilford and Simmons[10] and known ground state constants.[11] The difference between the B values derived with these two methods was smaller than the typical error for one determination ($\pm 0.0003\ \mathrm{cm}^{-1}$).

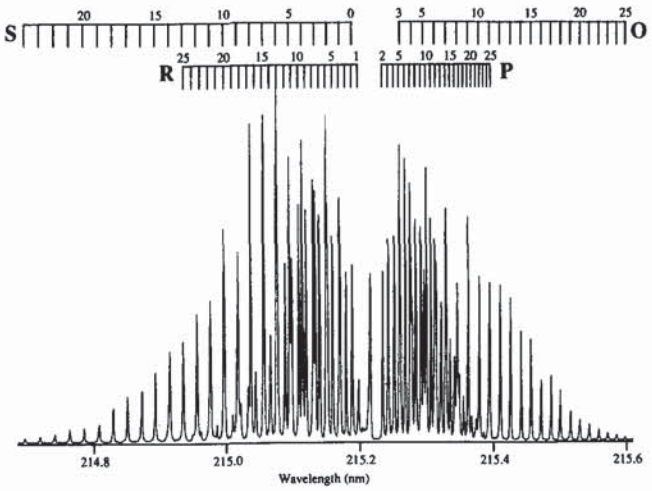

FIG. 1. 2 + 1 REMPI spectrum of room temperature CO at 8×10^{-8} Torr via the $E\ ^1\Pi$–$X\ ^1\Sigma^+$ (0,0) transition. This spectrum was obtained by monitoring the CO^+ ion signal.

III. RESULTS

A typical 2 + 1 REMPI spectrum of the CO $E\ ^1\Pi$–$X\ ^1\Sigma^+$ (0,0) band is shown in Fig. 1. This spectrum was taken in approximately 25 min with 2.8 mJ of light and a CO pressure of 8×10^{-8} Torr. The highest resolved rotational state in this spectrum was approximately 25. From this we estimated our detection sensitivity as approximately 3×10^6 molecules per quantum state per cm^3.

A. Rotational constants

Previous determinations of the E state rotational constants have all been from one-photon measurements.[5,6] Since the Q branch is unresolved at low J, the rotational constants were derived from only the e levels [i.e., from the (one-photon) P and R branches] of the $E\ ^1\Pi$ state. Because of this, only the B^e constant was measured. Our attempts to simulate the two-photon spectrum from the one-photon constants were completely unsuccessful, so we reevaluated these constants using the additional information gained from the two-photon spectrum.

For most Π states, the difference between B^f and B^e is quite small, and the average of the two is given. If, however, the state is perturbed by a neighboring Σ state, the situation is quite different. Because a sigma state has definite parity (Σ^+ is an e state, Σ^- an f state), only one of the Π lambda components will be perturbed. As discussed later, this perturbation changes the B constant of the perturbed lambda component. This effect is known as lambda doubling. If the perturber is a Σ^+ state, the lambda doubling parameter q is described by Eq. (1):

$$q = B_0^e - B_0^f, \tag{1a}$$

$$B_0 = B_0^f. \tag{1b}$$

If the perturber is a Σ^- state, the sign of q in Eq. (1a) is reversed, and B_0 is B_0^e. The B^e and B^f notation is more "natural" from an experimental viewpoint, while q is more useful in understanding the perturbation. This definition of q is consistent with Zare *et al.*[12]

In a two-photon process, five rotational branches are observed. Here, the O, Q, and S branches terminate on the e level of the E state, while the P and R branches terminate on the f level. We were thus able to measure the energies of both lambda doublets.

Our analysis assumed that the rotational energy of the E state was described by

TABLE I. Derived rotational constants for $E\,^1\Pi$ ($v=0$). All errors are 95% confidence limits.

B_0	$1.952\,64 \pm 0.000\,14\ \text{cm}^{-1}$
D_0	$6.00\times10^{-6} \pm 3.2\times10^{-7}$
q	$0.011\,86 \pm 0.000\,10$
B_0^f	$1.952\,64 \pm 0.000\,14$
B_0^e	$1.964\,50 \pm 0.000\,24$

$$E_{\text{rot}} = \begin{cases} (B_0 + q)J(J+1) - D_0J^2(J+1)^2 & (e \text{ levels}) \\ B_0J(J+1) - D_0J^2(J+1)^2 & (f \text{ levels}) \end{cases} . \quad (2)$$

This form assumes that the perturbing state is a Σ^+ state, as discussed later. The following constants were used to describe the $X\,^1\Sigma^+$ state:[11] $B_0 = 1.922\,528\,8\ \text{cm}^{-1}$, $D_0 = 6.121\times10^{-6}\ \text{cm}^{-1}$, and $H_0 = 5.74\times10^{-12}\ \text{cm}^{-1}$. The relative transition frequencies of the two-photon spectrum are completely determined by Eq. (2) and the ground state rotational constants; however, the exact frequencies are also dependent on the band origin ν_{00}.

The E state rotational constants were determined by fitting the observed transition frequencies to the assumed form. We performed a simultaneous nonlinear least-squares fit to all wavelengths using the Levenberg–Marquadt algorithm as implemented by Igor™ (WaveMetrics). The results are shown in Table I. Because our apparatus was not designed to measure absolute wavelengths, we did not attempt to determine ν_{00}. The rotational constants are dependent only on relative wavelengths. The quoted errors are 95% confidence limits based on five different recordings of the same spectrum. Blended lines were neglected in this analysis, so the positions of approximately 75 lines were used in each determination.

Our results are in excellent agreement with the one-photon measurements. We obtained a B_0^e of $1.9645 \pm 0.00024\ \text{cm}^{-1}$; other values in the literature are, for example, 1.9643,[7] 1.9645,[10] and $1.9644^{11}\ \text{cm}^{-1}$.

B. Power dependence

In order to characterize the 2 + 1 REMPI spectrum further, we measured the incident power dependence of the ion signal. The incident power was varied over the range of 3.5–0.30 mJ by attenuating both the doubled and the mixed UV light as necessary with either glass or quartz slides, respectively. Care was taken to avoid beam walk in doing this. We measured the intensities of a total of nine different transitions: $O(9)$, $O(10)$, $P(18)$, $R(14)$, $R(16)$, $R(19)$, $S(9)$, $S(19)$, and $S(20)$. Each transition was measured at approximately 25 different powers.

We found no branch-dependent or J-dependent effects. The resulting power curves were fit to the form I^n where I is the measured power. Our data were well fit to a curve of the form $I^{2.00\pm0.07}$. The quoted error is a 95% confidence limit. From this we conclude that the CO^+ ion signal displays a quadratic power dependence.

C. Intensities

The impetus behind this investigation was the need for a sensitive method for the quantitative detection of CO rotational state populations. In order to verify that this technique is truly quantitative, we measured the 2 + 1 REMPI spectrum of an ambient CO sample ($T\approx295$ K) under a range of powers. The resulting integrated intensities were then analyzed as described in this section and fit to a Boltzmann distribution.

The formal expression that describes a REMPI process is quite formidable; however, kinetic models often prove to be adequate for the prediction of ion yields.[13] In such a formalism, a 2 + 1 REMPI process is described by an initial absorption proceeding at a rate given by the product of a (J-dependent) cross section and the photon flux squared, while the second step would proceed at a rate that is linearly dependent on the photon flux. It is therefore often the case that the two-photon step is the rate-limiting step, and the contribution of the ionization photon can be neglected. The fact that we observed a quadratic power dependence suggests that this might be the case for the CO $E\,^1\Pi$–$X\,^1\Sigma^+$ transition.

If this assumption is true, the CO^+ ion yield, $N(J'',J')$, should be given by

$$N(J'',J') \propto I^2S(J'',J')P(J''), \quad (3)$$

where J'' is the ground rotational state, J' is the intermediate rotational state, $P(J'')$ is the ground state population, and $S(J'',J')$ is the two-photon line strength. These line strengths have a simple, algebraic form.[14] Because our laser power did not vary to an appreciable degree over the required range of wavelengths, we did not correct our populations for power and used only the two-photon line strengths to extract populations.

Figure 2 is a Boltzmann plot of our extracted popula-

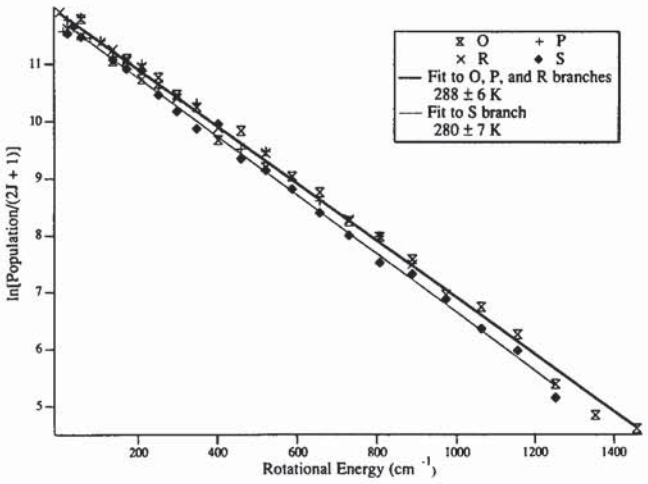

FIG. 2. Boltzmann plot of rotational populations derived from the spectrum in Fig. 1. The solid line indicates the best fit to a Boltzmann distribution. These data are best fit by a temperature of 283 K. The symbols denote the branch from which the data were obtained.

tions from the spectrum shown in Fig. 1. Typically, analysis of a single spectrum yields a temperature of 284 K with a standard deviation of 14 K. As illustrated in Fig. 2, the S branch of the spectrum gave consistently lower populations than the other three branches. Although the rotational distribution is well fit by a Boltzmann distribution, the derived ambient temperature is invariably too cold. This discrepancy is real and cannot be explained by statistical uncertainty. To illustrate this point, 12 spectra of ambient CO (temperature $\approx$295 K) were taken under essentially identical conditions. These spectra yielded temperatures from 270 to 291 K; each spectrum was consistently below room temperature. From this it is apparent that our sensitivity to the high rotational states must be less than that for low rotational states, thus leading to "cold" distributions.

D. Atomic ion channels

In addition to the CO^+ signal, another peak in the TOF spectrum was observed that had a charge-to-mass ratio of 12 and was hence assigned to C^+. A very small peak was sometimes observed with a charge-to-mass ratio of 16 and was attributed to O^+. Figure 3 shows a typical spectrum of these two channels.

The C^+ spectrum displays striking similarities to the CO^+ spectrum; however, they are not identical. Since the spectral features occur at the same wavelength, it is obvious that both are being produced by ionization of molecules prepared in the $E\,^1\Pi$ state. The intensity profiles of the two states are very different. The CO^+ spectrum has O and S branches of comparable magnitudes, while the S branch in the C^+ spectrum is almost twice as intense as the O branch. Figure 4 shows the relative production of C^+ vs CO^+ as a function of J' (E state rotational quantum number) and branch. C^+ formation is seen to be most important for high rotational states. Indeed, for $S(25)$ the CO^+ signal is only three times as intense as the C^+ signal.

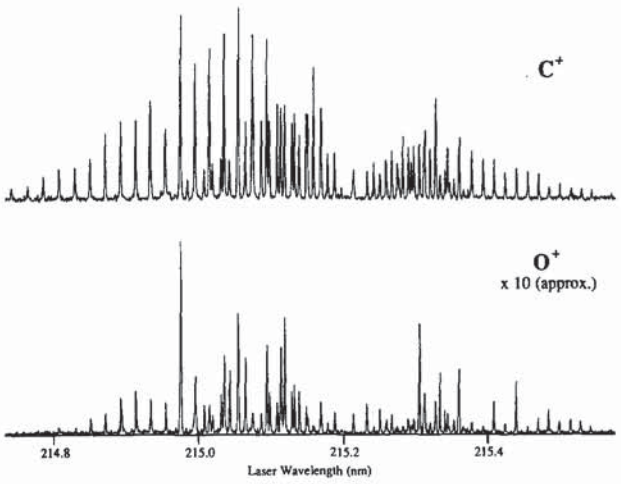

FIG. 3. 2 + 1 REMPI $E\,^1\Pi$–$X\,^1\Sigma^+$ (0,0) spectrum of room-temperature CO at 8×10^{-8} Torr. The upper spectrum was obtained by monitoring the C^+ ion and the lower by monitoring the O^+ ion. The lower trace has been expanded by approximately a factor of 10 for clarity.

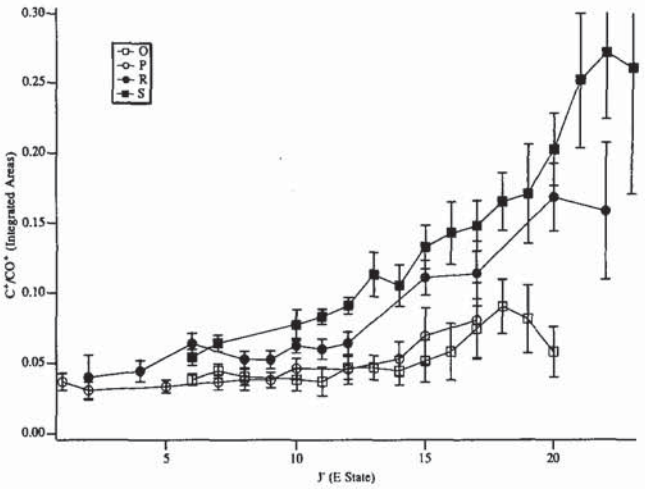

FIG. 4. C^+/CO^+ branching ratio as a function of J' (E state rotational quantum number). The symbols denote the branch from which the data were obtained.

It is clear that any one CO molecule cannot produce both a C^+ and a CO^+ ion, so an analysis of the ground state population distribution should take both channels into account. By neglecting the C^+ channel, as was done in our previous analysis, high rotational states were systematically undercounted. Because C^+ production is monotonically dependent on rotational state, this effect masqueraded as a cold temperature when only the CO^+ signal was analyzed. Additionally, since C^+ production is branch dependent, different branches had different apparent ground state populations.

In order to obtain correct ground state populations, contributions from both channels must be summed. When we performed this analysis on the same 12 spectra mentioned previously, we obtained an average temperature of 296 K with an average standard deviation of 15 K. The 12 temperatures ranged from 288 to 302 K. Additionally, agreement between the branches was improved. These results are summarized in Table II.

TABLE II. Comparison of temperatures obtained from a room-temperature ($T\approx$295 K) CO sample with and without the C^+ channel. The standard deviation of 12 determinations is given in parentheses. Note that the P and R branches are only partially resolved.

Branch	Only CO^+	$CO^+ + C^+$
All	284 (6.2) K	296 (4.8) K
S	274 (9.5)	294 (6.8)
R	303 (5.8)	318 (6.9)
P	301 (9.1)	307 (5.8)
O	275 (9.8)	281 (9.0)

A detailed analysis of the power dependence of the C^+ channel was not performed; however, some data on $S(19)$ and $S(20)$ were acquired. The C^+ signal from these two states was well fit by a power dependence of the form $I^{2.45\pm0.12}$. Unfortunately, this number does not shed any light on the dissociation process.

The O^+ signal is very weak; the most intense feature is two orders of magnitude less intense than the corresponding CO^+ peak. Additionally, the O^+ signal does not display the same smooth variation with J' and branch as the C^+ channel. Since the production of O^+ seems to be a very minor channel in these experiments, its role in the ionization of CO has been neglected.

IV. DISCUSSION

A. Quantitative detection of CO

We have shown that it is possible to obtain quantitative rotational populations for the ground state of CO using the $2+1$ REMPI spectrum of the CO $E\,^1\Pi$–$X\,^1\Sigma^+$ transition. For this, it is desirable to measure not only the CO^+ signal, but also the C^+ signal. If the distribution to be measured has only a modest amount of rotational excitation, the error introduced by not accounting for the C^+ signal may be acceptable. This is illustrated in Table II. The measured temperature of a 295 K sample of CO is about 10 K too low if only the CO^+ signal is used. The small error in this measurement, about 4%, is somewhat misleading, because the highest rotational states in this sample are undercounted by 20% (as seen in Fig. 4)! If the distribution to be measured is rotationally hot, the C^+ signal should not be neglected, as this will most certainly lead to artifacts.

B. Production of C^+

Without a detailed knowledge of the repulsive states of CO^+, it is impossible to identify the processes that produce C^+; however, some guesses may be made based upon the energetic constraints. The lowest energy pathway that leads to atomic ions is the $C^+ + O$ channel, which requires 22.35 eV. The other channel, $C + O^+$, requires 24.7 eV. Using photons of approximately 5.75 eV, there are a number of energetically allowed pathways leading to $C^+ + O$ but not to $C + O^+$. For example, a $2+2$ absorption through the E state [Fig. 5(a)] leaves the system approximately 23 eV above the ground state—enough to form C^+ but not O^+. This process, although energetically allowed, is probably not competitive with the formation of CO^+ ion, because the latter is a $2+1$ process.

A second possibility is that ions formed in the X state of CO^+ absorb more photons, leading to the production of C^+ as illustrated in Fig. 5(b). Absorption of one photon from the $v=0$ level of the X state is still 2.5 eV below the required energy to produce C^+ ions. It is unlikely that high vibrational states of the CO^+ X state are formed, because the E state of CO belongs to a Rydberg series converging on the CO^+ X state. A two-photon absorption from the X state would be above the barrier for both O^+ and C^+ production.

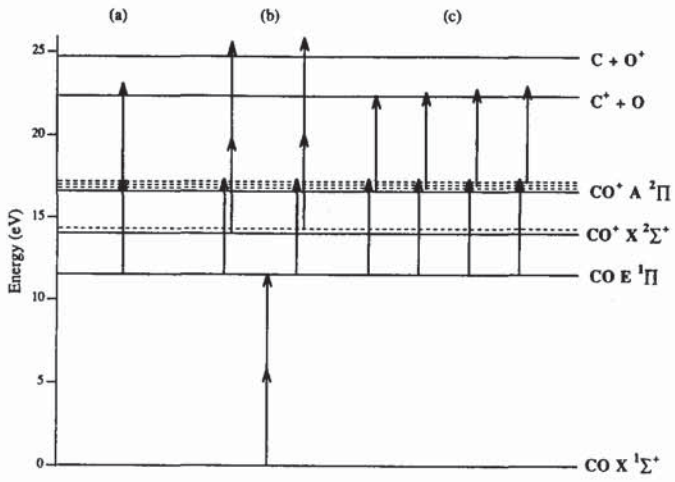

FIG. 5. Possible paths leading to the production of atomic ions. The dotted lines indicate excited vibrational states. The ionization step has been slightly offset for clarity. (a) $2+2$ ionization and photodissociation. (b) $2+1$ REMPI to the CO^+ X state followed by two-photon absorption leading to photodissociation. (c) $2+1$ REMPI to the CO^+ A state followed by a one-photon absorption leading to photodissociation.

The most likely source of C^+ ions is CO^+ ions formed in the A state [see Fig. 5(c)]. Energetically, a one-photon absorption from the E state of CO may form ions in up to $v=3$ of the CO^+ A state. Since the A state is a valence state and has a vibrational spacing significantly different from the CO E state, these $\Delta v \neq 0$ transitions should have significant Franck–Condon overlap.

There is evidence in the literature that some CO^+ ions are formed in the A state. In their investigation of the $2+1$ REMPI of CO through the E state, Fujii, Ebata, and Ito[4] observed fairly strong fluorescence after their pump pulse. They attributed this fluorescence to the CO $E\,^1\Pi$–$A\,^1\Sigma^+$ transition; however, the steady-state population of the E state is expected to be rather small because of the high probability of subsequent ionization. Additionally, the $E\,^1\Pi$–$A\,^1\Sigma^+$ transition has a quantum efficiency of 1%.[8] For these reasons, it seems more likely that they observed fluorescence from the CO^+ $A\,^2\Pi$–$X\,^2\Sigma^+$ transition. Because of the short lifetime of the CO $E\,^1\Pi$ state, a lifetime study of the fluorescence should resolve this point.

From Fig. 4, it is obvious that C^+ production is a function of both rotational energy and branch. The branch dependence is most likely an energetic effect. For example, the O and S branches of the spectrum access the same levels of the E state; however, they require quite different wavelengths to do so (as illustrated in Fig. 1). Because of this, more photodissociation channels may be available to the S branch, as it lies at shorter wavelengths. The adiabatic energy for $C^+ + O$ production is almost exactly resonant with a $2+1+1$ absorption through the E state of CO and then the $v=0$ level of the A state of CO^+. It is possible that only some parts of the E state spectrum (e.g., parts of the R and S branches) have enough energy to form C^+ via the $v=0$

level of the A state; however, uncertainties in the dissociation limit of CO make this impossible to calculate with any precision. This would explain why these branches have significantly higher C^+ production.

The rotational state dependence of C^+ ion formation is more intriguing. Since all four branches seem to show increasing C^+ formation as a function of J, this effect is not purely energetic in nature. Additionally, if the molecules were being excited directly to a repulsive state of CO^+, rotational effects would be minimal. It is possible that some of the pathways to C^+ formation proceed via a predissociative state of CO^+. At least four excited states of CO^+ are known to predissociate to $C^+ + O$.[11]

The monotonic increase of C^+ ions with J' suggests two possible types of predissociation. The first is predissociation by rotation.[15] Since rotational predissociation is caused by tunneling through the centrifugal barrier, it displays a marked dependence on rotational state. Although this type of predissociation is consistent with the observed J dependence, it is hard to believe that tunneling is a significant process in a molecule as heavy as CO. The second type of predissociation is gyroscopic predissociation.[16] This type of predissociation also has a marked J dependence because the coupling to the dissociative state is caused by the operator

$$B(r)(J_+ L_- + J_- L_+). \tag{4}$$

Additionally, so long as neither the predissociative state nor the dissociative state is a $^2\Sigma$ state, both lambda doublets (and hence all branches) would be affected.

Without more information on the excited states of CO^+, both bound and repulsive, it is impossible to do more than speculate about the nature of these interactions. More than likely, there are a number of pathways open for each transition. Additionally, the relative importance of each pathway may be influenced by laser intensity. One strategy to avoid measuring the C^+ channel would be to calibrate the CO^+ channel against a known distribution (such as a thermal distribution); however, any such calibration would be dependent on laser power and related parameters such as focusing and beam quality.

As more and more intense lasers become readily available, other MPI systems that display problems of this nature are likely to be found. Indeed, at higher powers the O^+ channel in this system will undoubtedly become important. Because of this, the common assumption that ionization processes are independent of rotational state must be regarded as suspect. For example, we studied the $2+2$ REMPI detection of CO via the $A\ ^1\Pi$ state, but found that this system was particularly vexed by branch-dependent, power-dependent, and J-dependent effects.

C. Lambda doubling and perturbing states

The large lambda doubling in the E state, almost 5 cm^{-1} at $J = 20$, is the most striking feature of the spectrum. In this case, the perturbation appears to be predominantly due to the neighboring $C\ ^1\Sigma^+$ state. Both of these states are Rydberg states belonging to the same nl complex. The E state is nominally the $3p\pi$ state, while the C state is the $3p\sigma$ state. Similar lambda doubling effects[17] have been seen in the $c\ ^3\Pi$ state, which is also the $3p\pi$ state. In order to test whether the major perturber is the C state, we can estimate the magnitude of the perturbation by assuming that the $E\ ^1\Pi$ and $C\ ^1\Sigma^+$ wave functions are well approximated by atomic orbitals. This may seem to be a crude approximation, especially for an $n = 3$ Rydberg state; however, the point of the calculation is to explain, not predict, the lambda doubling. Additionally, SCF calculations of these states show that, at least near equilibrium, these states are predominantly Rydberg in nature.[18]

The term in the Hamiltonian that is responsible for lambda doubling is

$$-\frac{1}{2\mu r^2}(J_+ L_- + J_- L_+), \tag{5}$$

where μ is the reduced mass of CO, r is the internuclear distance, and $J_\pm$, $L_\pm$ are the raising/lowering operators for total angular momentum and electronic angular momentum, respectively. Because L is odd under reflection through a plane containing the internuclear axis, it is apparent that this Hamiltonian will connect states of opposite symmetry. Since the $C\ ^1\Sigma^+$ level has e symmetry, only the e levels of the $E\ ^1\Pi$ state will be perturbed. This parity-selective perturbation causes the appearance of the lambda doubling parameter q in Eq. (2).

The perturbing part of the Hamiltonian leads to matrix elements of the form

$$\langle v'| -\frac{1}{2\mu r^2} |v\rangle \langle 3p\lambda' | J_+ L_- + J_- L_+ | 3p\lambda \rangle,$$
$$\lambda = \sigma, \pi^+, \pi^-. \tag{6}$$

Since we assumed a particularly simple basis set, the angular part of this expression is readily evaluated. The vibrational term is a bit more difficult. Formally, the $v = 0$ level of the E state is perturbed by every vibrational level of the C state. Both the $v = 0$ and $v = 1$ levels of the $C\ ^1\Sigma^+$ state are close to the $E\ ^1\Pi$ $(v = 0)$ level; the $C\ ^1\Sigma^+$ $(v = 0)$ level lies 985 cm^{-1} below the $E\ ^1\Pi$ $(v = 0)$ level while the $C\ ^1\Sigma^+$ $(v = 1)$ level is 1190 cm^{-1} above it. The other vibrational levels are much more distant. Because of this, we only included contributions from the $v = 0$ and 1 levels of the C state in our calculation. Further details of the calculation are described in the Appendix.

The leading term in the perturbed energy is proportional to $J(J+1)$. The proportionality factor is q, the lambda doubling parameter. Using these approximations, we obtained the expression

$$q = 4B_0^2 \left[\frac{1}{E_{\Pi} - E_{\Sigma, v=0}} + \frac{1}{138(E_{\Pi} - E_{\Sigma, v=1})} \right], \tag{7}$$

where $E_{\Pi}, E_{\Sigma, v=0}$, and $E_{\Sigma, v=1}$ are the energies of the $E\ ^1\Pi$ $(v = 0, J = 1)$, $C\ ^1\Sigma^+$ $(v = 0, J = 0)$, and $C\ ^1\Sigma^+$ $(v = 1, J = 0)$ levels, respectively. This leads to a predicted lambda doubling parameter of $q = 0.015$ cm^{-1}, which agrees satisfactorily with the experimentally observed value of 0.011 86 cm^{-1}. Our overestimation of the degree of lambda doubling is no doubt due to the assumption of atomic wave functions. Any departure from an ideal Rydberg state

would lower the atomic character of the wave function and hence decrease the magnitude of the perturbation. The unusual magnitude of the lambda doubling parameter is directly related to the proximity of the $C\,^1\Sigma^+$ ($v=0$) level. Although the $C\,^1\Sigma^+$ ($v=1$) level also contributes, it is approximately two orders of magnitude less important.

In our analysis, we have neglected the contributions from states other than the C state for two reasons. The first is that the C state is 5000 cm^{-1} closer to the E state than the next closest Σ state, the $B\,^1\Sigma^+$ state. Since the perturbation is inversely proportional to the energy splitting of the two states [see Eq. (7)], this means the perturbation from the B state will be at least six times smaller than that of the C state. The second reason it that the perturbation from other states will be much smaller because they do not belong to the same nl complex as the E state. In order for another state to affect the lambda doubling of the E state, it must either have some $3p\sigma$ character or the E state must have some character of another atomic state. This can be seen from the second term of Eq. (6). Since the E and C states seem to be well represented by the atomic wave functions, other states must correspondingly have little character of this type.

In our expression for the rotational energies of the E state, we explicitly assumed that the centrifugal distortion parameter (D) was identical for both lambda doublets. As with the effective B constants, this is an oversimplification. We have also neglected in our analysis a term known as the centrifugal distortion to the lambda doubling parameter q_D. We estimated the value of this parameter using the same approximations as for q and obtained

$$q_D = 16B_0^4 \frac{1}{(E_{\Pi} - E_{\Sigma,v=0})^3}. \tag{8}$$

In this expression, all terms which contribute less than half of a percent were omitted. From this, q_D is expected to be 2.4×10^{-7} cm^{-1}. When we included the discrepancy between our calculated and observed values of q in this estimate, we obtained a more reliable estimate of 1.5×10^{-7} cm^{-1}. Since both of these estimates are smaller than our estimated error in D_0, any attempt to derive q_D from our data would have been unfounded.

V. CONCLUSIONS

We have shown that it is possible to obtain quantitative, rotationally resolved populations for CO ($v=0$) with a detection limit of approximately 3×10^6 molecules per quantum state per cm^3 by $2+1$ REMPI through the $E\,^1\Pi$ state. The ground state rotational population can be obtained from this technique; however, both CO^+ and C^+ ions must be collected for reliable, quantitative measurements. Failure to account for the C^+ channel systematically undercounts the higher rotational levels. For samples that show modest amounts of rotational excitation, such as room temperature samples, failure to account for the C^+ channel leads to errors on the order of 20% for high J's ($J\approx20$). For samples with significantly more rotational excitation, neglect of the C^+ channel could be much more serious. From our data, we were also able to obtain new rotational constants for the $E\,^1\Pi$ state that show a large lambda doubling, ascribed to a perturbation by the nearby $C\,^1\Sigma^+$ state.

Note added in proof: Dispersed fluorescence measurements show that CO^+ is formed in both the A and X states in $2+1$ REMPI of CO through the $E\,^1\Pi$ state (Taka Ebata, private communication).

ACKNOWLEDGMENTS

We would like to thank Taka Ebata for sending us a copy of Ref. 4 prior to publication. M.A.H. would like to thank Jon Gutow for calibrating the etalon used for wavelength calibration. H.A.M. would like to thank Stacey F. Shane for her assistance in our first recording of the CO REMPI spectrum, and Jinchun Xie, Dahv A. V. Kliner, and Andrew C. Kummel for helpful suggestions. This work was funded by the Office of Naval Research under Contract No. N00014-87K-0204.

APPENDIX

In order to calculate the amount of lambda doubling in the $v=0$ level of the $E\,^1\Pi$ state due to the $v=0,1$ levels of the $C\,^1\Sigma^+$ level, we assumed a Hamiltonian of the form

$$H = H_{\text{elec,vib}} + H_{\text{rot}} - \frac{1}{2\mu r^2}(J_+ L_- + J_- L_+), \tag{A1}$$

and diagonalized the resulting 3×3 matrix to obtain the required energies. Since $L_\pm$ is actually a sum over one-electron operators, we were able to neglect contributions from all orbitals besides the ones in question.

The electronic basis set was composed of the $3p$ atomic orbitals in the proper symmetry combinations:

$$|^1\Sigma^+\rangle = |3p\sigma_0\rangle,$$
$$|^1\Pi_e\rangle = \frac{1}{\sqrt{2}}[\,|3p\pi^1_{-1}\rangle + |3p\pi^1_1\rangle\,]. \tag{A2}$$

Both the C and E states of CO are fairly harmonic. We thus used the harmonic oscillator basis functions to form the vibrational basis set. Additionally, the resonant frequencies of the two states differ by less than half a percent, so we neglected this difference. The necessary vibrational matrix elements are thus[19]

$$\left\langle 0\left|\frac{1}{2\mu r^2}\right|0\right\rangle = \frac{1}{\hbar^2}B_0,$$
$$\left\langle 0\left|\frac{1}{2\mu r^2}\right|1\right\rangle = 0.085\,\frac{1}{\hbar^2}B_0. \tag{A3}$$

In evaluating these matrix elements, we used our measured value of B_0 for the E state. Because the C state is perturbed by the E state, the measured values of B_v for the C state contain contributions from lambda doubling and are not the true B_v values.

The eigenvalues of the resulting matrix were then obtained to second order in $J(J+1)$. The first-order term was identified as q, the lambda doubling parameter, while the second order term is the so-called centrifugal distortion of q, q_D. As expected, the centrifugal distortion is negligible for all observed rotational states and does not become important until very high rotational levels are considered.

[1] J. W. Hepburn, F. F. Northrup, G. L. Ogram, and J. C. Polanyi, Chem. Phys. Lett. **85**, 127 (1982).
[2] D. A. Mantell, S. B. Ryali, G. L. Haller, and J. B. Fenn, J. Chem. Phys. **78**, 4250 (1983).
[3] I. Burak, J. W. Hepburn, N. Sivakumar, G. E. Hall, G. Chawla, and P. L. Houston, J. Chem. Phys **86**, 1258 (1987).
[4] A. Fujii, T. Ebata, and M. Ito, Chem. Phys. Lett. **161**, 93 (1989).
[5] J. J. Hopfield and R. T. Birge, Phys. Rev. **29**, 922 (1927).
[6] S. G. Tilford, J. T. Vanderslice, and P. G. Wilkinson, Can J. Phys. **43**, 450 (1965).
[7] S. Ogawa and M. Ogawa, J. Mol. Spectrosc. **49**, 454 (1974).
[8] C. Letzelter, M. Eidelsberg, F. Rostas, J. Breton, and B. Thieblemont, Chem. Phys. **114**, 273 (1987).
[9] W. H. Smith, Phys. Scr. **17**, 513 (1978).
[10] S. G. Tilford and J. D. Simmons, J. Phys. Chem. Ref. Data **1**, 147 (1972).
[11] K. P. Huber and G. Herzberg, *Molecular Spectra and Molecular Structure IV. Constants of Diatomic Molecules* (Van Nostrand Reinhold, New York, 1979), pp. 162–171.
[12] R. N. Zare, A. L. Schmeltekopf, W. Harrop, and D. L. Albritton, J. Mol. Spectrosc. **46**, 37 (1973).
[13] D. H. Parker, in *Ultrasensitive Laser Spectroscopy*, edited by D. S. Kliger (Academic, Orlando, 1983), p. 233.
[14] R. G. Bray and R. M. Hochstrasser, Mol. Phys. **31**, 1199 (1976).
[15] G. Herzberg, *Molecular Spectra and Molecular Structure I. Spectra of Diatomic Molecules* (Van Nostrand Reinhold, New York, 1950), pp. 425–430.
[16] H. Lefebvre-Brion and R. W. Field, *Perturbations in the Spectra of Diatomic Molecules* (Academic, Orlando, 1986), p. 360.
[17] M. L. Ginter and S. G. Tilford, J. Mol. Spectrosc. **31**, 292 (1969).
[18] D. L. Cooper and K. Kirby, J. Chem. Phys. **87**, 424 (1987).
[19] H. Lefebvre-Brion and R. W. Field, in Ref. 16, p. 144.